PHENIX measurements of elliptic and triangular flow in small systems

Victoria Greene, for the PHENIX Collaboration
Vanderbilt University, Nashville, TN

PHENIX
Venezia 2018 Quark Matter

Abstract

Results on azimuthal anisotropies in the particle production from p+p and $p/d/^3$He+A at LHC and RHIC have raised the question of how small a system can be while still exhibiting collective behavior. RHIC operations have included p+Au, d+Au, and ^{3}He+Au collisions at $\sqrt{s_{NN}} = 200$ GeV and d+Au collisions at $\sqrt{s_{NN}} = 200$, 62.4, 39, and 19.6 GeV. In this poster we present PHENIX results on elliptic and triangular flow at midrapidity as a function of transverse momentum and pseudorapidity in d+Au collisions. We compare these results with several theoretical predictions in scenarios including viscous hydrodynamic flow, partonic scattering, and purely hadronic scattering in order to assess the origin of collectivity in the smallest systems.

Geometry Studies

Collision initial geometry is determined by proton shape fluctuations, intrinsic nucleus shape, impact parameter, and the distribution of nucleon-nucleon collisions on an event-by-event basis. The small systems geometry scan at RHIC collided $p/d/^3$He+Au to make intrinsic nucleus shape the dominant factor when comparing these three systems.

Small Systems Geometry Study at RHIC

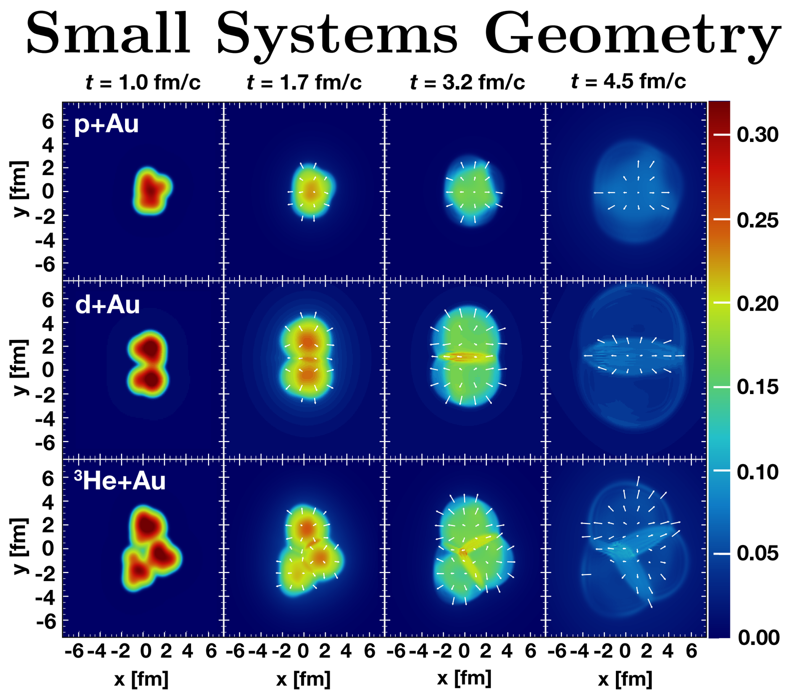

Fig. 1: SONIC evolution of characteristic head-on $p/d/^3$He+Au collision at $\sqrt{s_{NN}} = 200$ GeV. Each row gives the temperature distribution of the nuclear matter at four time points following the initial collision at $t = 0$. [1]

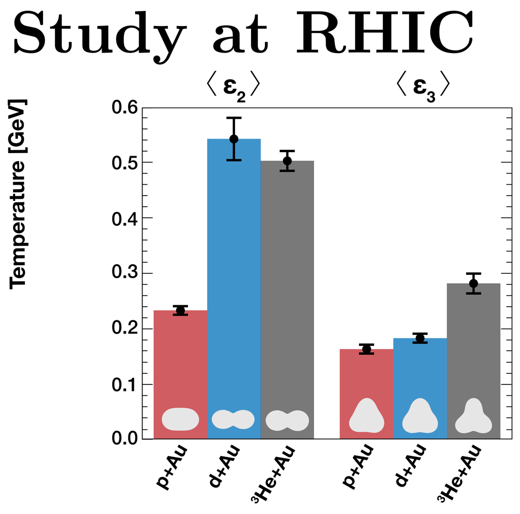

Fig.2: Monte Carlo Glauber calculation for eccentricity of the initial state. [1]

$$\varepsilon_n = \frac{\sqrt{\langle r^n \cos(n\phi)\rangle^2 + \langle r^n \sin(n\phi)\rangle^2}}{\langle r^n \rangle}$$

PHENIX Detector

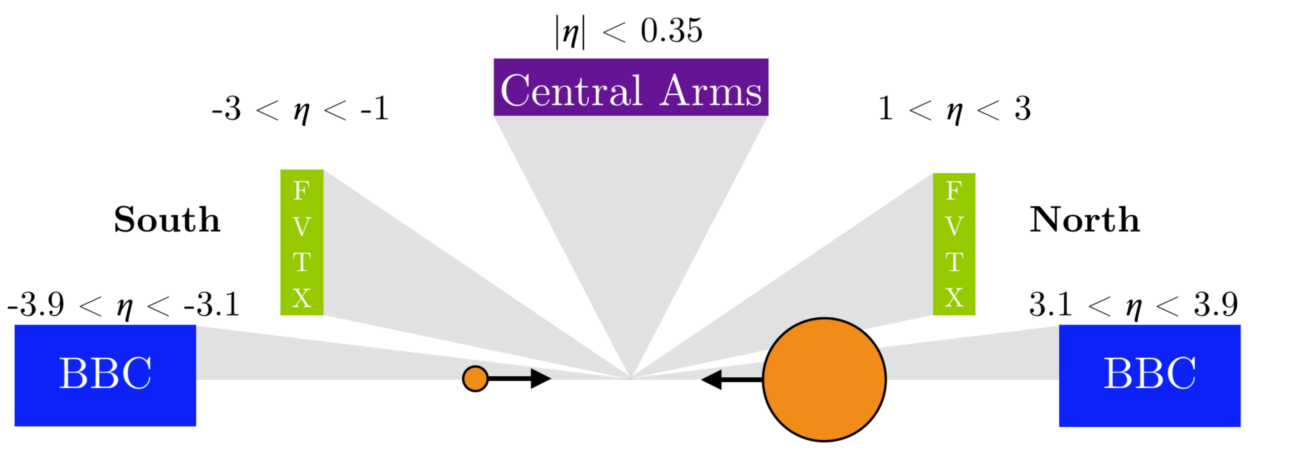

Fig. 3: Cartoon of PHENIX geometry.

The event plane angle is measured in the FVTX south and BBC south. The azimuthal distribution of charged particles are measured in the central arms at midrapidity.

$$\frac{dN}{d\phi} \propto 1 + \sum_n 2v_n(p_T)\cos(n(\phi - \psi_n))$$

The event plane resolution is measured with the 3 subevent method using the BBC, FVTX, and central arm. Analysis done in south (Au-going) side to optimize resolution.

Analysis Method

This poster shows results found using the event plane method. Additional measurements using the cumulants method can also be found in Ref. [2].

$v_2(p_T)$ and $v_3(p_T)$ in Small Systems

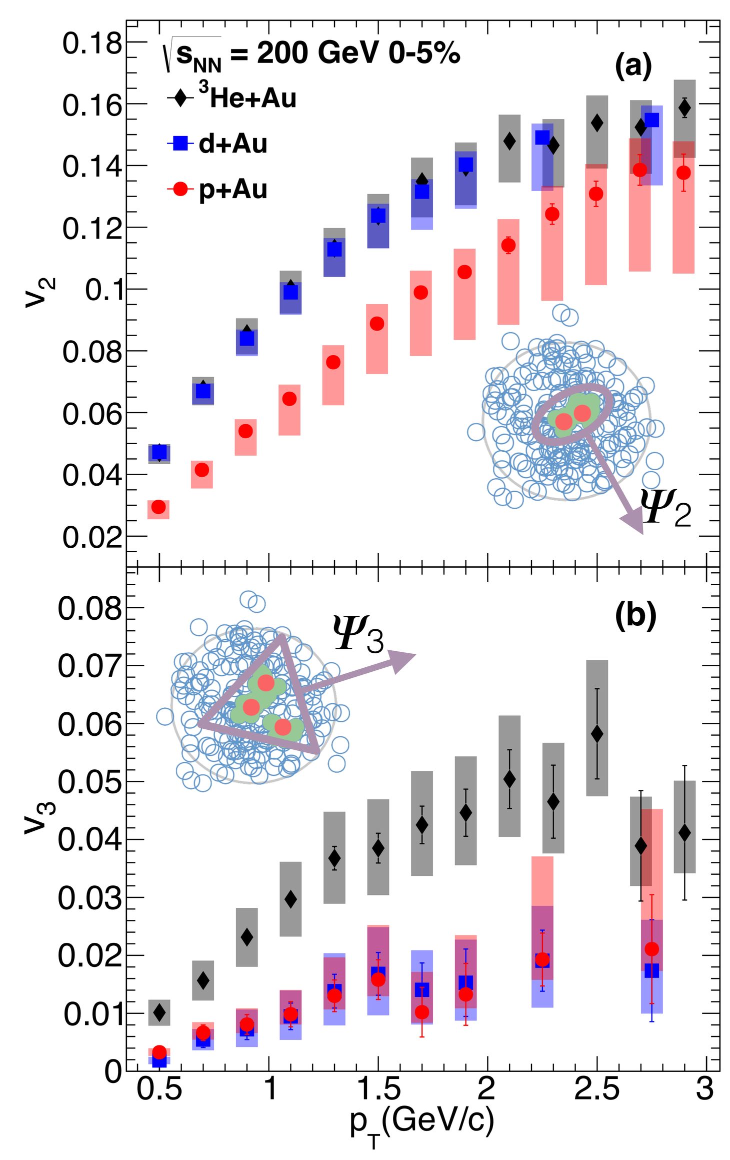

Fig. 4: (a) $v_2(p_T)$ and (b) $v_3(p_T)$ $p/d/^3$He+Au. [1]

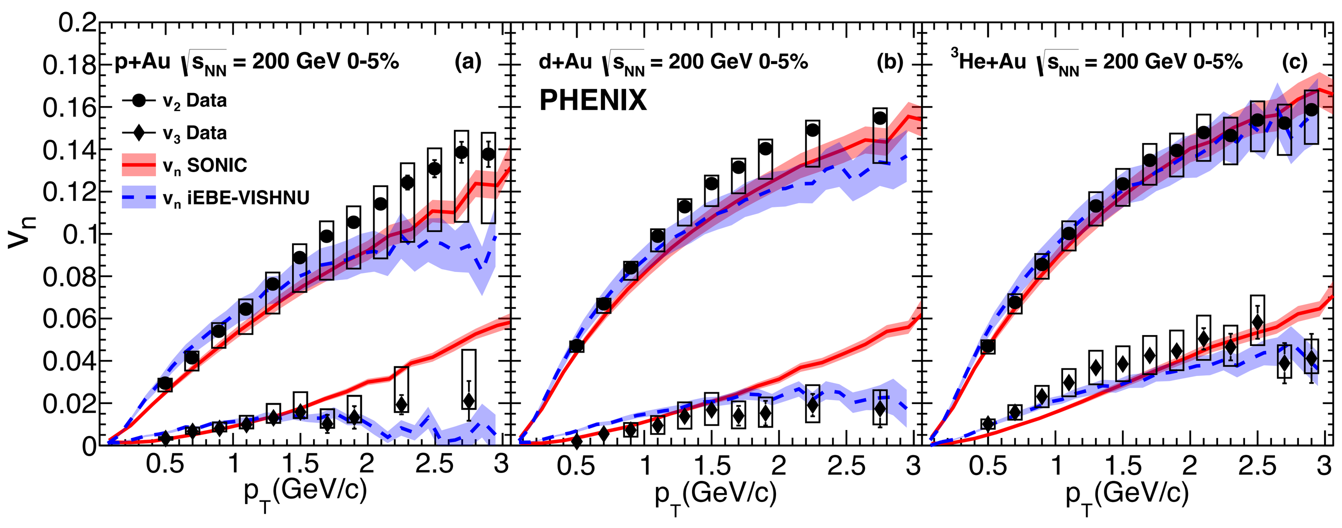

Fig. 5: SONIC (solid) and iEBE-VISHNU (dashed) model calculations compared to $v_2(p_T)$ and $v_3(p_T)$ in (a) p+Au (b) d+Au, and (c) ^{3}He+Au. [1]

Ordering of $v_2(p_T)$ and $v_3(p_T)$ matches ordering of average initial-state eccentricities according to a Monte Carlo Glauber model, suggesting an efficient translation of initial-state spatial anisotropies into final-state momentum anisotropies. Data agreement with hydrodynamic models SONIC and iEBE-VISHNU support this interpretation.

$$v_2^{p+\mathrm{Au}} < v_2^{d+\mathrm{Au}} \approx v_2^{^3\mathrm{He+Au}}$$
$$v_3^{p+\mathrm{Au}} \approx v_3^{d+\mathrm{Au}} < v_3^{^3\mathrm{He+Au}}$$

Beam Energy Scan $v_2(p_T)$ and $v_2(\eta)$ in d+Au

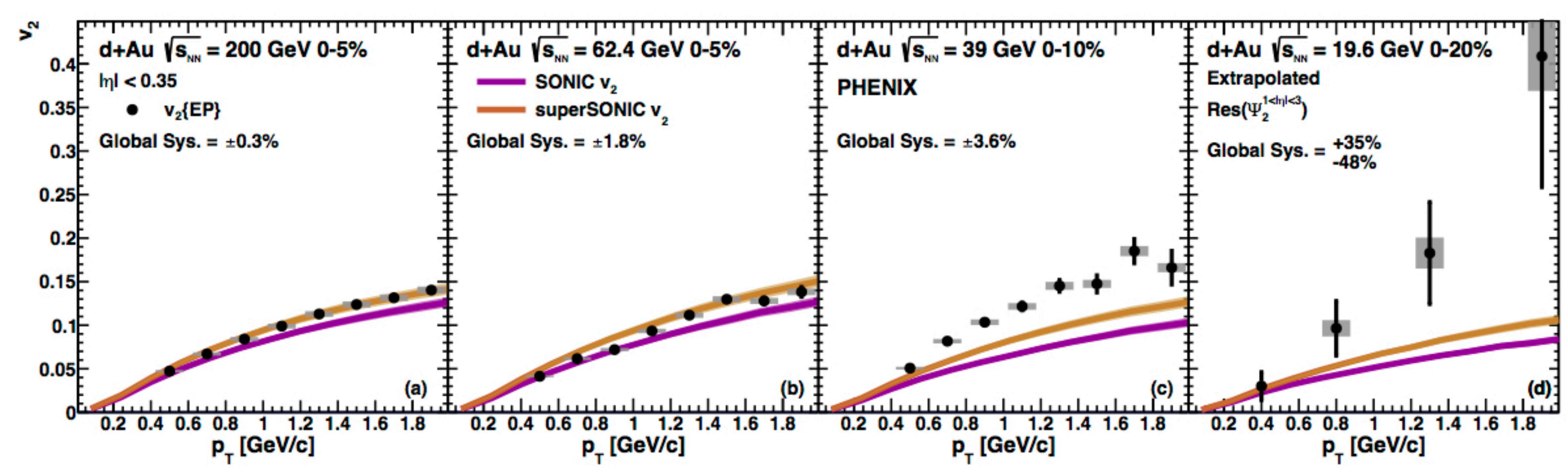

Fig. 6: $v_2(p_T)$ from hydrodynamics and data. [2]

Hydrodynamic models describe the measured signal at high energies. At low energies the models fall below the measurement.

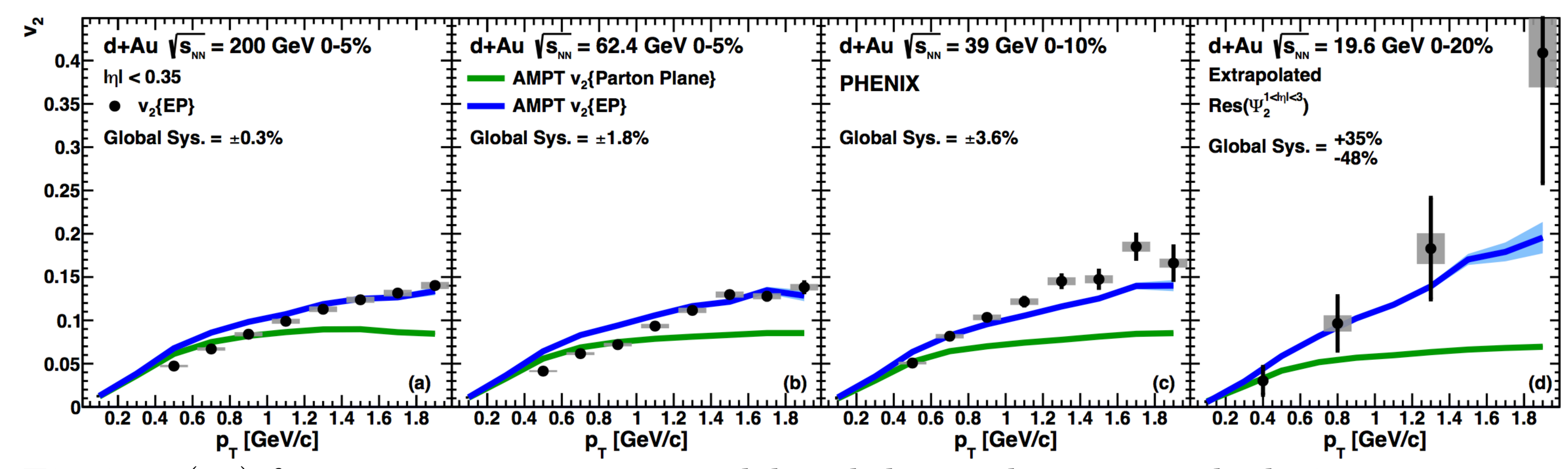

Fig. 7: $v_2(p_T)$ from parton transport model and data. The AMPT calculation was analyzed with the parton plane (green) and event plane (blue) methods.[2]

Event plane calculation is similar to the measurement at all energies. The parton plane is true flow, while the event plane analysis includes nonflow contributions (as do the data).

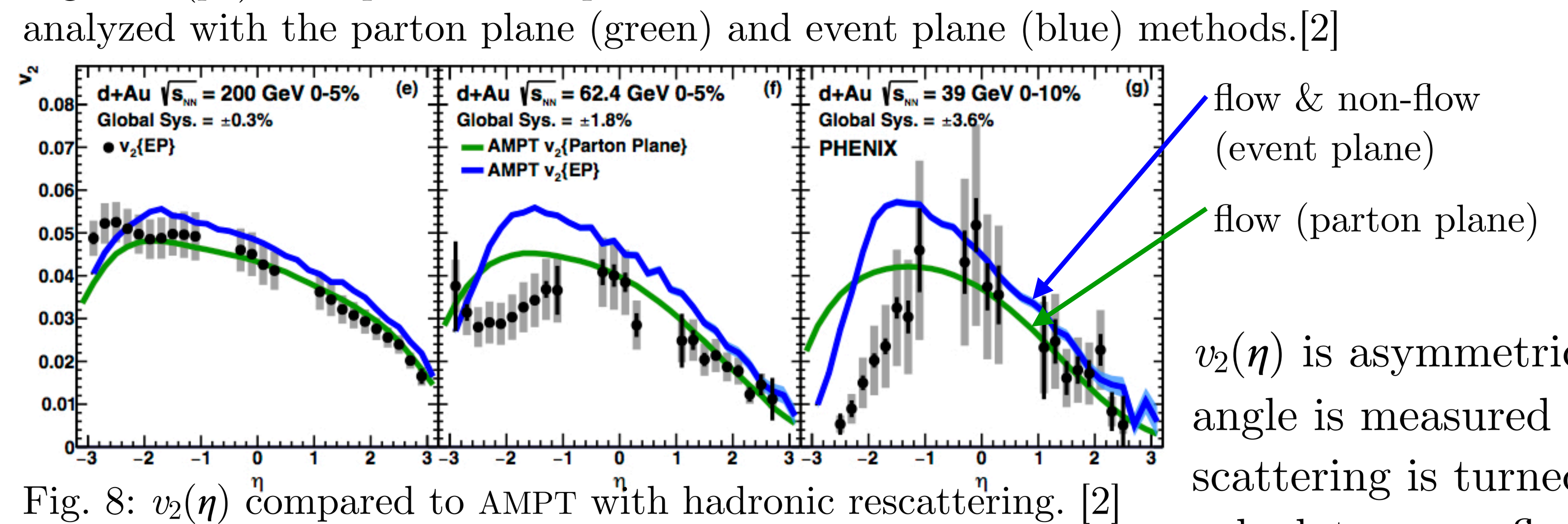

Fig. 8: $v_2(\eta)$ compared to AMPT with hadronic rescattering. [2]

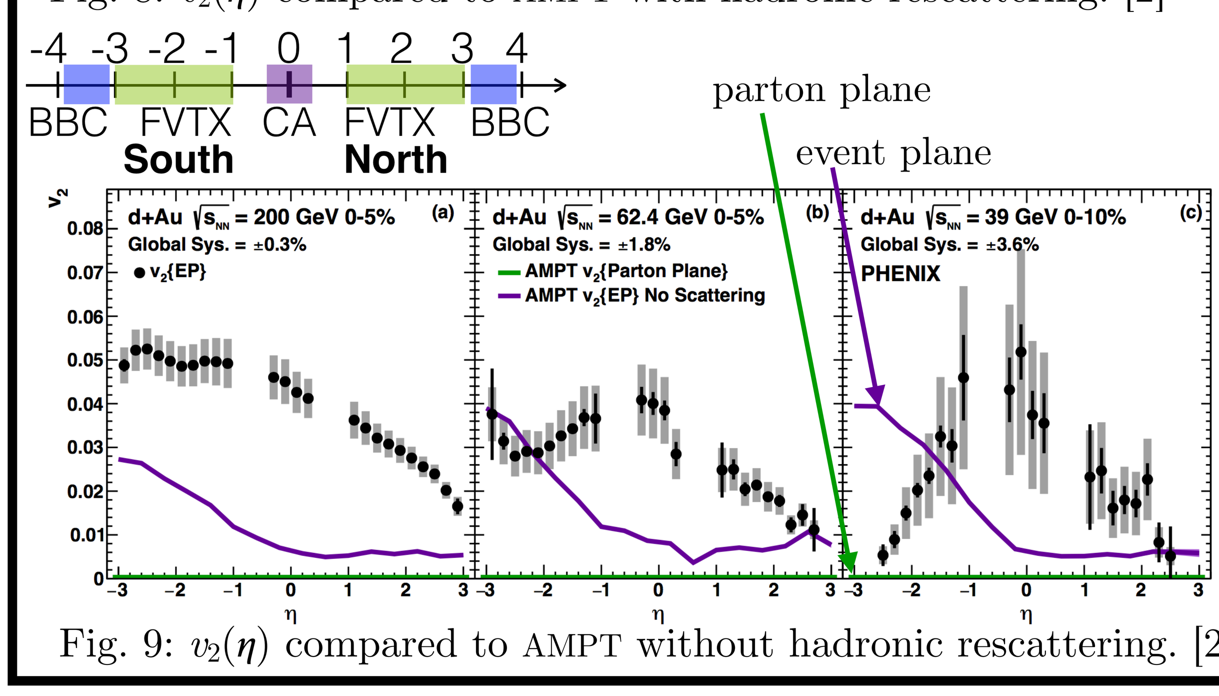

Fig. 9: $v_2(\eta)$ compared to AMPT without hadronic rescattering. [2]

$v_2(\eta)$ is asymmetric, and the event plane angle is measured in the BBC. When scattering is turned on, the parton plane calculates pure flow and the event plane calculates the flow and nonflow combination. Removing partonic and hadronic scattering removes all correlations related to the initial geometry so that flow equals zero leaving the event plane calculation to be pure nonflow. The pure flow and pure nonflow do not simply add to equal the flow and nonflow combination.

Conclusion

The small systems geometry scan shows matched ordering of ⟨ε$_n$⟩ to $v_n(p_T)$ and a simultaneous description of $v_2(p_T)$ and $v_3(p_T)$ by hydrodynamics. This suggests the presence of a strongly coupled fluid in small systems. $v_2(p_T)$ is measured at all energies in the beam energy scan in d+Au. Nonflow contributions are more prominent at lower energies. $v_2(\eta)$ is measured as an asymmetric signal. The shape is similar for all energies at $\eta > 0$. Combination of flow and non-flow is not simply additive.

BROOKHAVEN NATIONAL LABORATORY

[1] arXiv:1805.02973
[2] *Phys. Rev. C* **96**, 064905 (2017) (arXiv:1708.06983)

VANDERBILT UNIVERSITY